Electronic Supplementary Material (ESI) for ChemComm.

Supplementary Material (ESI) for:

Double Spin Crossovers: A New Double Salt Strategy to Improve Magnetic and Memory Properties

Wasinee Phonsri[a], Barnaby A. I. Lewis[a,b], Guy N. L. Jameson[c] and Keith S. Murray[a*]

[a] School of Chemistry, 17 Rainforest Walk, Monash University, Clayton, VIC 3800, Australia

[b] Department of Chemistry, University of Warwick, Coventry CV4 7AL, UK

[c] School of Chemistry, Bio21 Molecular Science and Biotechnology Institute, 30 Flemington Road, The University of Melbourne, Parkville, VIC 3010, Australia

E-mail: keith.murray@monash.edu

General

All reagents and solvents were purchased from Sigma–Aldrich and used as received. Infrared spectra were measured with a Bruker Equinox 55 FTIR spectrometer fitted with a 71Judson MCT detector and Specac Golden Gate diamond ATR. Mass spectrometry analyses were performed using electrospray ionization mass spectra (ESI-MS) and were recorded with a Micromass (now Waters) ZMD with Waters alliance e2695 HPLC system for automatic sample injections. MeOH was the mobile phase and had a flow rate of 100 µL min^{-1}. Microanalyses were performed by Elemental Analysis Service, London Metropolitan University, London, UK. TGA measurement was performed using a MettlerTGA/DSC 1 thermal analysis instrument at a heating rate of 5 °C min^{-1}.Differential Scanning Calorimetry data was examined using DSC Q100 V9.9 Build 303 using aluminium pan at a heating/cooling rate of 10 °C min^{-1}. Variable-temperature magnetic susceptibility data were collected with a Quantum Design MPMS XL superconducting quantum interference device (SQUID) magnetometer, in sweep mode with a scan speed of 10 and 5 K min^{-1}. X-ray powder diffraction patterns were recorded with a Bruker D8 Advance powder diffractometer operating at Cu Kα wavelength (1.5418 Å), with samples mounted on a zero-background silicon single crystal stage. Scans were performed at room temperature in the 2θ range 5–55°.

Mössbauer spectra were recorded on a spectrometer from SEE Co. (Science Engineering & Education Co., MN) equipped with a closed cycle refrigerator system from Janis Research Co. and SHI (Sumitomo Heavy Industries Ltd.). Data were collected in constant acceleration mode in transmission geometry. The zero velocity of the Mössbauer spectra refers to the centroid of the room temperature spectrum of a 25 µm metallic iron foil. Analysis of the spectra was conducted using the WMOSS program (SEE Co, formerly WEB Research Co. Edina, MN). The lowest temperature was investigated first, the sample then warmed to the next temperature followed by a 10 minute thermal equilibration time and the spectrum then measured over at least 24 hours.

X-ray crystallographic measurements on **1** at 100 K were collected at the Australian Synchrotron operating at approximately 16 keV (λ = 0.71073 Å). The collection temperature was maintained at specified temperatures using an open-flow N_2 cryostream. Data were collected using Blue Ice software [1]. Initial data processing was carried out using the XDS package [2]. The CCDC number is 1917674.

X-ray crystallographic measurements on **1**, at 300 and 370 K, were collected using a XtaLAB Synergy, Dualflex, HyPix diffractometer with Cu-*K*α radiation (*λ* = 1.54184Å). Single crystals were mounted on a glass fibre using super glue. The data collection and integration were performed within CrysAlisProsoftware programs and corrected for absorption using CrysAlisPro 1.171.39.46 (Rigaku Oxford Diffraction, 2018). The CCDC numbers are 1917673 and 1922394, for the structure at 300 and 370 K, respectively. These data are provided free of charge by The Cambridge Crystallographic Data Centre. For the 370 K structure, checkCif alert level B, C52 and C54, response is 'hydrogen atoms associated with partially occupied acetonitrile solvent have not been included'.

Synthesis of $K[Fe^{III}(azp)_2]\cdot(H_2O)_3\cdot MeOH$

The method followed that of Takahashi *et al.*[3] although that group obtained crystals with a different solvate composition and different crystallographic packing to that obtained here. See ref 6 for further details.

2,2'-dihydroxoazobenzene (0.43 g, 2 mmol) was suspended in ethanol (10 ml) to which potassium hydroxide (0.24 g, 4.4 mmol) dissolved in ethanol (8 ml) was added, resulting in a black/brown solution. This solution was added, dropwise, to a solution of $FeCl_3$ (162 mg, 1 mmol) in ethanol (5 ml). This black/brown solution was left stirring overnight then filtered. After evaporation of the solvent from the filtrate a black, shiny powder was formed. This powder was recrystallised from a solution of methanol (7 ml) and diethylether (7 ml) to yield black crystals in 75% yield (470 mg).$\tilde{u}_{max}/cm^{-1}$2922 (ν_{Ar-H}), 1648 ($\nu_{C=N}$),1585 ($\nu_{C=C}$), 1317 (ν_{C-N}), 1284 (ν_{C-O}).ESI-MS: m/z = 480 $[Fe(azp)_2]^-$. Crystallography (*vide infra*) showed the crystals to be $K[Fe^{III}(azp)_2]\cdot(H_2O)_3\cdot MeOH$. Microanalysis on a bulk sample suggested the loss of methanol and water of solvation; calc. for $K[Fe(azp)_2]\cdot H_2O$ (found %) $C_{24}H_{18}FeKN_4O_5$: C, 53.64 (52.82); H, 3.38 (3.45); N, 10.43 (10.31).

Synthesis of $[Fe(3,5\text{-}Me_2TPM)(TPM)][ClO_4]_2$

To prepare $[Fe(3,5\text{-}Me_2TPM)(TPM)][ClO_4]_2$, the same method as was used to synthesize $[Fe(3,5\text{-}Me_2TPM)(TPM)][BF_4]_2$[4] was applied,with $Fe(ClO_4)_2\cdot nH_2O$ used instead of $Fe(BF_4)_2\cdot 6H_2O$.

3,5-Me_2TPM (0.298 g, 1.00 mmol)[5] was dissolved in acetonitrile (30 ml) to give a clear, brown solution. A clear yellow solution of Iron(II) perchlorate hexahydrate (0.373 g, 1.00 mmol) in acetonitrile (5 ml) was added dropwise. After five hours of stirring, TPM (0.214 g, 1 mmol)[6] was added to the solution causing a colour change to form a slightly darker brown. The solution was filtered after 20 mins of stirring, leaving a pink solid (0.027 g), which is $[Fe(TPM)_2][ClO_4]_2$[6]on the filter paper. The brown filtrate was evaporated to 50% volume using a rotary evaporator. The remaining brown filtrate was filtered again and left to slowly evaporate at room temperature. After one week, red block-like crystal were obtained (137 mg, 18% yield).$\tilde{u}_{max}/cm^{-1}$1560, 1271, 1252 cm^{-1} for 3,5-Me_2TPM; 1514, 1316, 1274 cm^{-1} for TPM. ESI-MS: m/z = 568 $[Fe(3,5\text{-}Me_2TPM)(TPM)]^{2+}$, 99 $[ClO_4]^-$. PXRD diffractograms on a bulk sample, compared to that simulated from the single crystal structure, are shown in Fig S8.

Table S1 Crystallographic data and structure refinement of **1**

[Fe(3,5-Me_2TPM)(TPM)][Fe(azp)$_2$]ClO_4·Sol	**Sol = 2MeCN**	**2MeCN**	**MeCN**
	100 K	**300 K**	**370 K**
Formula	$C_{54}H_{54}ClFe_2N_{18}O_8$	$C_{54}H_{54}ClFe_2N_{18}O_8$	$C_{52}H_{51}ClFe_2N_{17}O_8$
Molecular weight / $gmol^{-1}$	1230.30	1230.30	1189.21
Crystal system	Monoclinic,	Monoclinic,	Monoclinic,
Space group	$P2_1/c$	$P2_1/c$	$P2_1/c$
a / Å	16.948 (3)	17.2097 (8)	17.2993 (8)
b / Å	10.425 (2)	10.5679 (3)	10.5858 (4)
c / Å	31.438 (6)	32.232 (2)	32.3862 (14)
α / °	90	90	90
β / °	100.41 (3)	101.230 (5)	101.594 (4)
γ / °	90	90	90
Cell volume / $Å^3$	5463 (2)	5749.8 (5)	5809.8 (4)
Z	4	4	4
Absorption coefficient / mm^{-1}	0.653	0.621	4.979
Reflections collected	89605	66647	40838
Independent reflections,R_{int}	14724, 0.0338	19255, 0.0765	11855
Max. and min. transmission	0.993 and 0.977	0.21322 and 1.00000	0.29224 and 1.00000
Restraints/parameters	0/794	3/794	10/802
Final R indices [$I>2\sigma(I)$]: R_1, wR_2	0.0445, 0.1211	0.0593, 0.1878	0.0815, 0.2681
CCDC number	1917674	1917673	1922394

Table S2 Selected bond lengths and octahedral distortion parameters for MeCN solvates of **1**. Fe1 is the Fe^{III} anion while Fe2 is the Fe^{II} cation

	2MeCN	**2MeCN**		**MeCN**
	100 K	**300 K**		**370 K**
Fe1-O1/Å	1.902 (2)	1.916 (2)	Fe1-O1/Å	1.954 (4)
Fe1-O2/Å	1.886 (2)	1.885 (2)	Fe1-O2/Å	1.921 (4)
Fe1-O3/Å	1.9088 (18)	1.920 (2)	Fe1-O3/Å	1.942 (4)
Fe1-O4 Å	1.8849 (19)	1.874 (3)	Fe1-O4, Fe1-O4'/Å	2.01 (3), 1.903 (15)
Fe1-N1, Fe1-N1'/Å	1.942 (3), 1.917 (3)	2.028 (7), 1.954 (8)	Fe1-N1, Fe1-N1'/Å	2.117 (11), 2.046 (16)
Fe1-N3, Fe1-N3'/Å	1.925 (3), 1.926 (4)	2.059 (8), 1.907 (8)	Fe1-N3, Fe1-N3'/Å	2.160 (14), 2.01 (3)
Fe2—N5/Å	1.9792 (15)	2.087 (2)	Fe2—N5/Å	2.136 (4)
Fe2—N6/Å	1.9874 (15)	2.116 (2)	Fe2—N6/Å	2.167 (3)
Fe2—N7/Å	1.9944 (16)	2.106 (2)	Fe2—N7/Å	2.150 (3)
Fe2—N8/Å	1.9656 (16)	2.119 (2)	Fe2—N8/Å	2.165 (4)
Fe2—N9/Å	1.9772 (16)	2.136 (2)	Fe2—N9/Å	2.188 (4)
Fe2—N10/Å	1.9617 (15)	2.094 (2)	Fe2—N10/Å	2.150 (4)
Σ/° (Fe1, Fe2)[a]	51, 23	55, 54	Σ/° (Fe1, Fe2)	60, 66
Θ/° (Fe1, Fe2)[b]	113, 36	147, 68	Θ/° (Fe1, Fe2)	183, 82

[a] Σ^o = the sum of |90-θ| for the 12 N-Fe-N/N-Fe-O angles in the octahedron. [b] Θ^o = the sum of |60-θ| for the 24 N-Fe-N/N-Fe-O angles describing the trigonal twist angle.

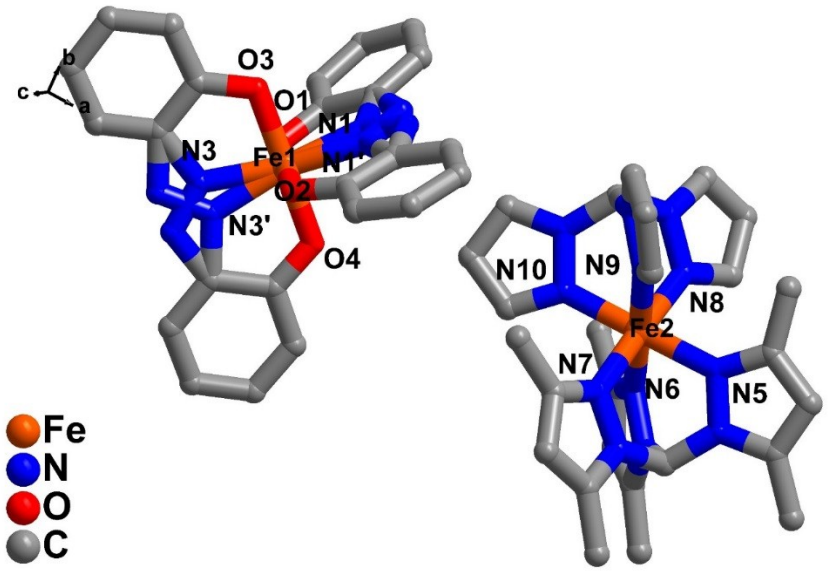

Figure S1 The asymmetric unit of **1** with atomic label on donor atoms surrounding metal centers. Hydrogen atoms, a perchlorate anion and acetronitrile solvates are omitted for clarify.

Table S3 Selected intermolecular interactions in **1** at 100, 300 and 370 K

	100 K	**300 K**	**370 K**
a chain of Fe^{II} along *b* axis			
C50-H50···O5	2.3535(4)	2.3353(1)	2.2842(1)
C46-H46···O6	2.5435(5)	2.6783(1)	2.6403(1)
C47-H47···O6	2.4967(5)	2.6160(1)	2.7142(1)
C50-H50···O7	2.3140(4)	2.5140(1)	(2.7498(1))
C43-H43···O7	2.4863(4)	2.4440(1)	2.5413(1)
C43-H43···O8	2.5209(4)	2.9136(2)	(3.1827(1))
along *a* axis			
C48-H48···O4	2.6022(6)	(2.8222(1))	(3.0112(1))
C41-H41···π	2.713	2.985	(3.060)
C29-H29B···O1	2.4696(4)	2.6558(1)	2.7113(1)
π···π	3.662	3.695	3.689
along *c* axis			
C45-H45···O2	2.6182(4)	2.6301(1)	2.6424(1)
C39-H39B···π	2.866	2.804	2.865
MeCN			
C54-H54C···O1	2.5751(4)	(2.7778(1))	-
C52-H52A···O3	2.5234(5)	(2.8467(1))	-
C54-H54B···π	2.981	2.975	-
C52-H52C···N18	2.6760(9)	(2.8407(2))	-
C29-H29A···N17	2.5917(5)	2.7045(1)	-

Note: MeCN solvent molecules are disordered at 370 K. All interactions relating to the solvents then are not considered.

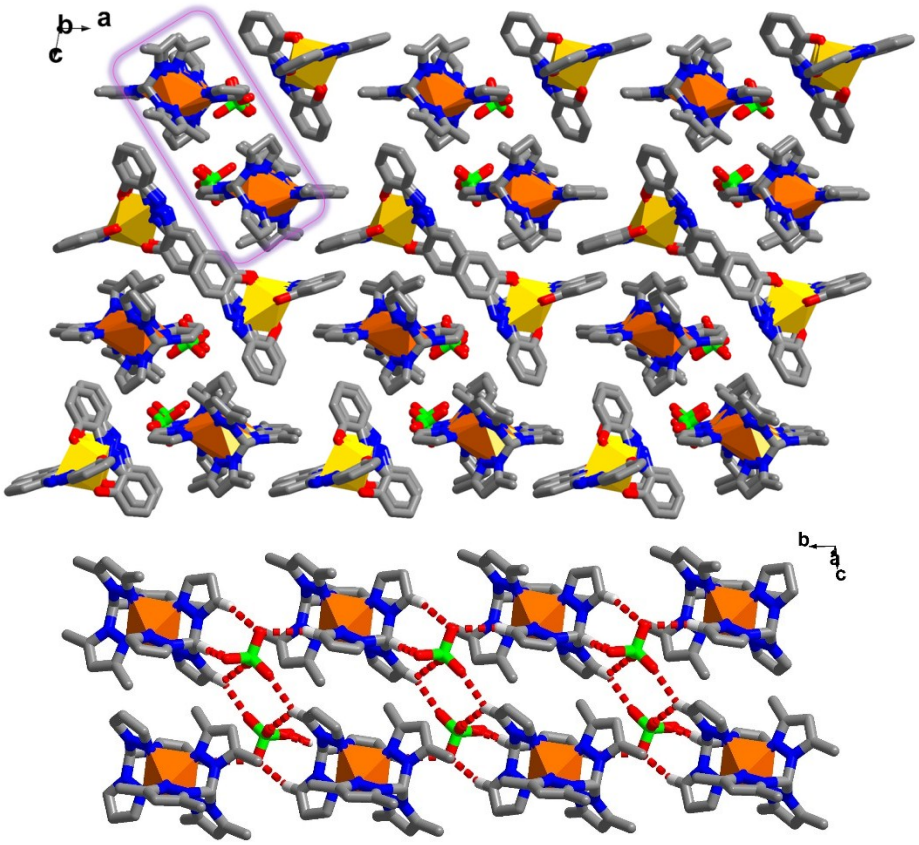

a

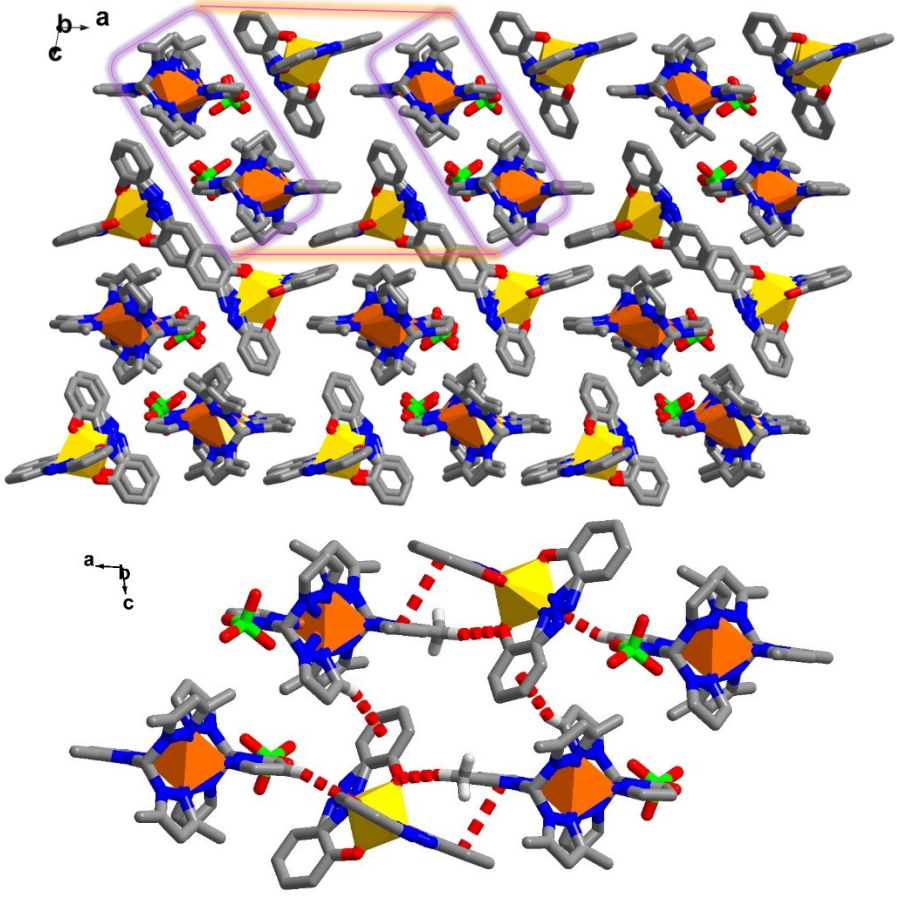

b

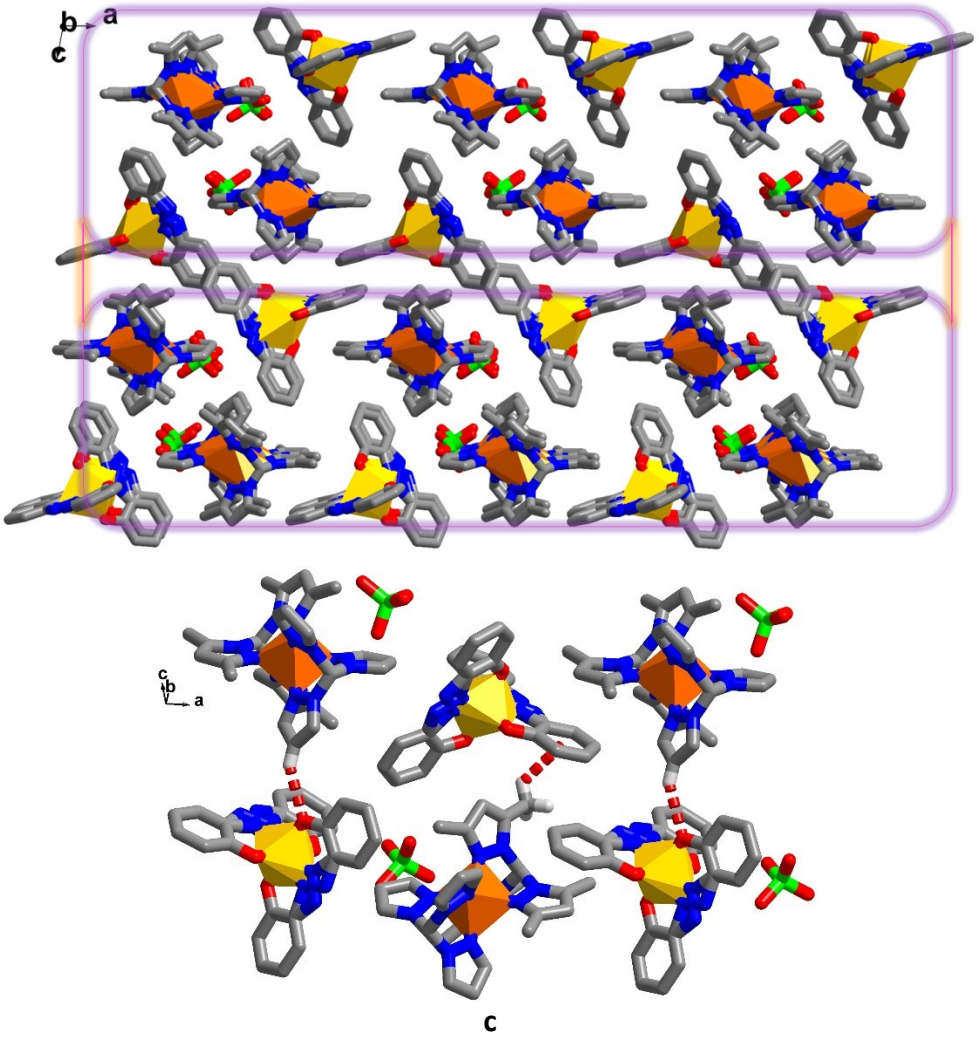

Figure S2 Crystal packing for **1** shows a) the formation of Fe^{II} double chain with ClO_4^- anions *via* C-H···O (ClO_4^-) interactions along the *b* axis, b) C-H···π/O and π-π interactions between the Fe^{II} double chain with adjacent $[Fe^{III}(azp)_2]^-$ molecules along the *a* axis giving rise to a Fe^{II}-Fe^{III} double sheet and c) C-H···π/O interactions between Fe^{II} and Fe^{III} molecules from neighbouring sheets resulted in the *pseudo*-3D structure of **1**.

Table S4 Crystallographic data and structure refinement of [Fe(3,5-Me_2TPM)(TPM)][ClO_4]$_2$·

[Fe(3,5-Me_2TPM)(TPM)][ClO_4]$_2$·	**100 K**	**300**
Formula	$C_{26}H_{32}Cl_2FeN_{12}O_8$	$C_{26}H_{32}Cl_2FeN_{12}O_8$
Molecular weight / gmol^{-1}	767.38	767.38
Crystal system	Monoclinic	Monoclinic
Space group	$P2_1$	$P2_1$
a / Å	8.1900 (16)	8.2600 (17)
b / Å	10.350 (2)	10.470 (2)
c / Å	18.920 (4)	19.280 (4)
α / ^{o}	90	90
β / ^{o}	94.13 (3)	94.32 (3)
γ / ^{o}	90	90
Cell volume / Å^3	1599.6 (6)	1662.6 (6)
Z	2	2
Absorption coefficient / mm^{-1}	0.708	0.681
Reflections collected	32246	34806
Independent reflections,R_{int}	9260, 0.0230	9815, 0.0512
Max. and min. transmission	0.986 and 0.967	0.986 and 0.968
Restraints/parameters	1/448	1/449
Final R indices [$I>2\sigma(I)$]: R_1, wR_2	0.0401, 0.103	0.0515, 0.1597
CCDC number	1942808	1942807

Table S5 Selected bond lengths and octahedral distortion parameters for [Fe(3,5 Me_2TPM)(TPM)][ClO_4]$_2$

	100 K	**300 K**
Fe2—N1/Å	1.978 (3)	2.039 (3)
Fe2—N3/Å	1.992 (3)	2.054 (4)
Fe2—N5/Å	1.989 (3)	2.054 (4)
Fe2—N7^i/Å	1.976 (3)	2.064 (4)
Fe2—N9/Å	1.969 (3)	2.040 (4)
Fe2—N11/Å	1.968 (3)	2.034 (4)
Σ/° (Fe1, Fe2)	26	43
Θ/° (Fe1, Fe2)	35	52

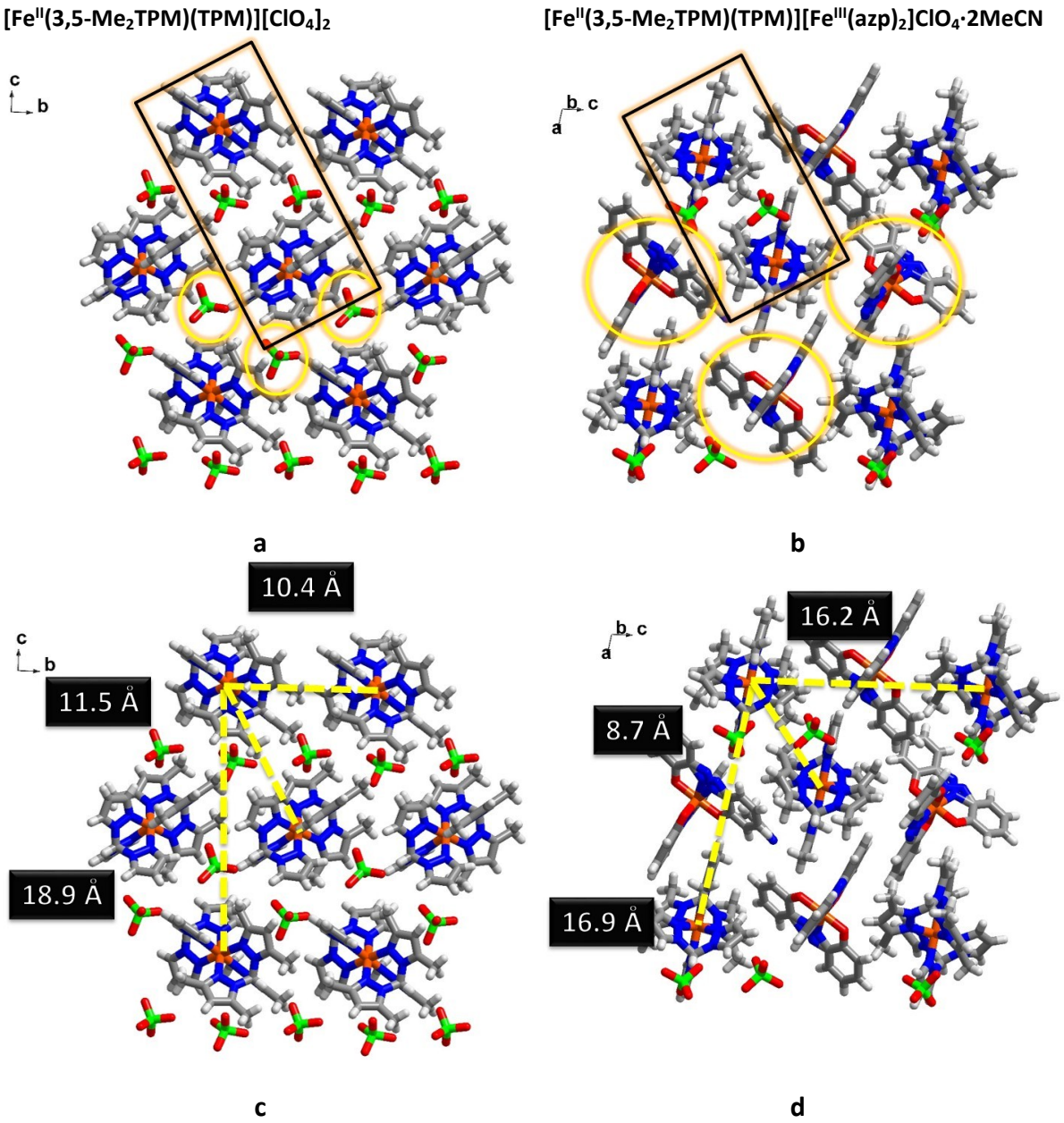

Figure S3 Similar crystal packing in the cationic precusor, [Fe^{II}(3,5-Me$_2$TPM)(TPM)][ClO$_4$]$_2$ and in [Fe^{II}(3,5-Me$_2$TPM)(TPM)][Fe^{III}(azp)$_2$]ClO$_4$·2MeCN, **1**. Yellow cirlcles in a) and b) showing [Fe^{III}(azp)$_2$]$^-$ molecules occupying similar pockets as one of the ClO$_4^-$ in [Fe^{II}(3,5-Me$_2$TPM)(TPM)][ClO$_4$]$_2$. Fe^{II}···Fe^{II} distances for c) [Fe^{II}(3,5-Me$_2$TPM)(TPM)][ClO$_4$]$_2$ and d) compound **1**.

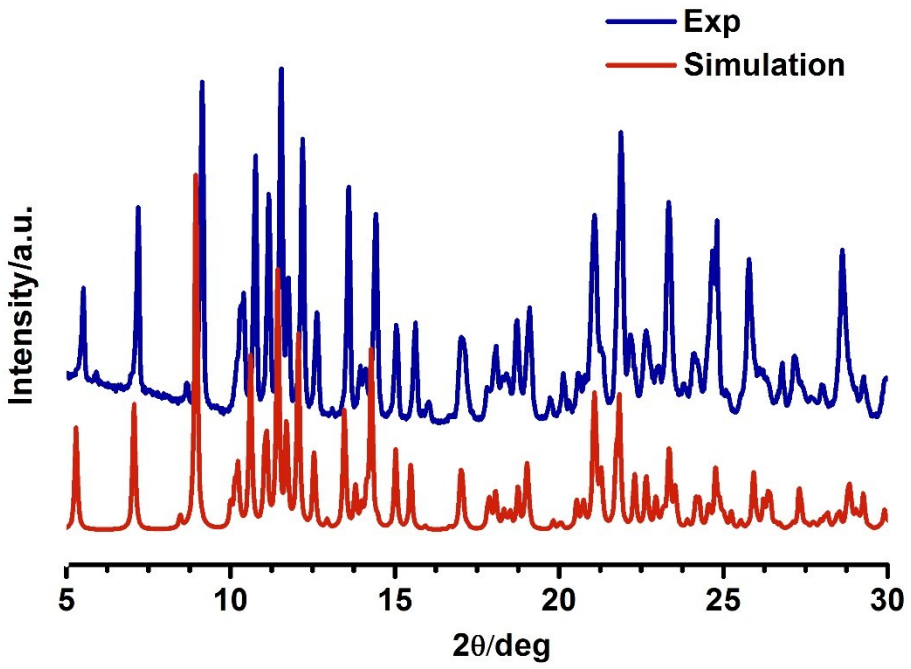

a

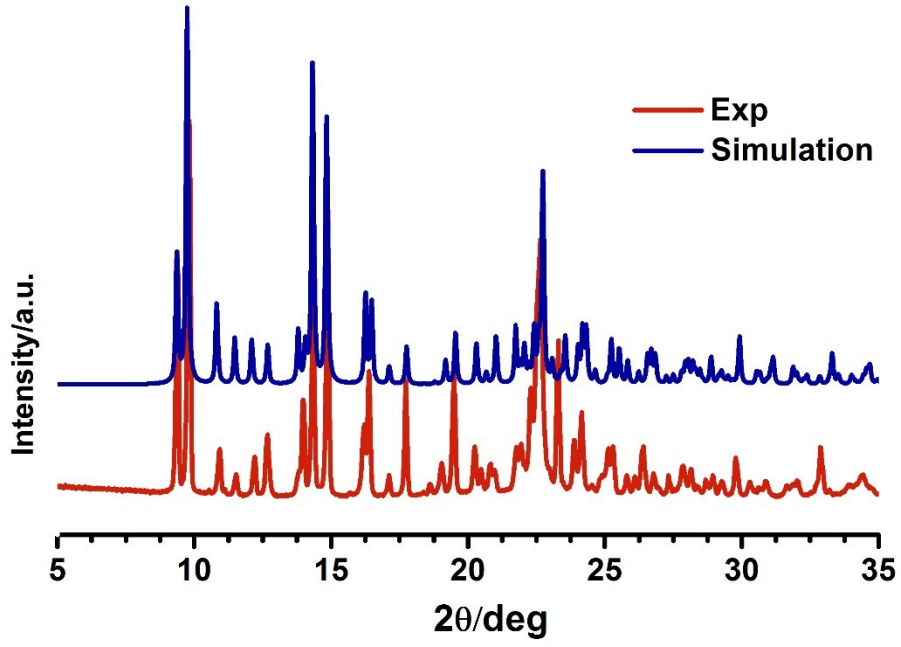

b

Figure S4 PXRD of bulk sample of a) **1** and b) precursor [Fe(3,5-Me_2TPM)(TPM)][ClO_4]$_2$ comparing to the simulated single crystal X-ray diffraction data.

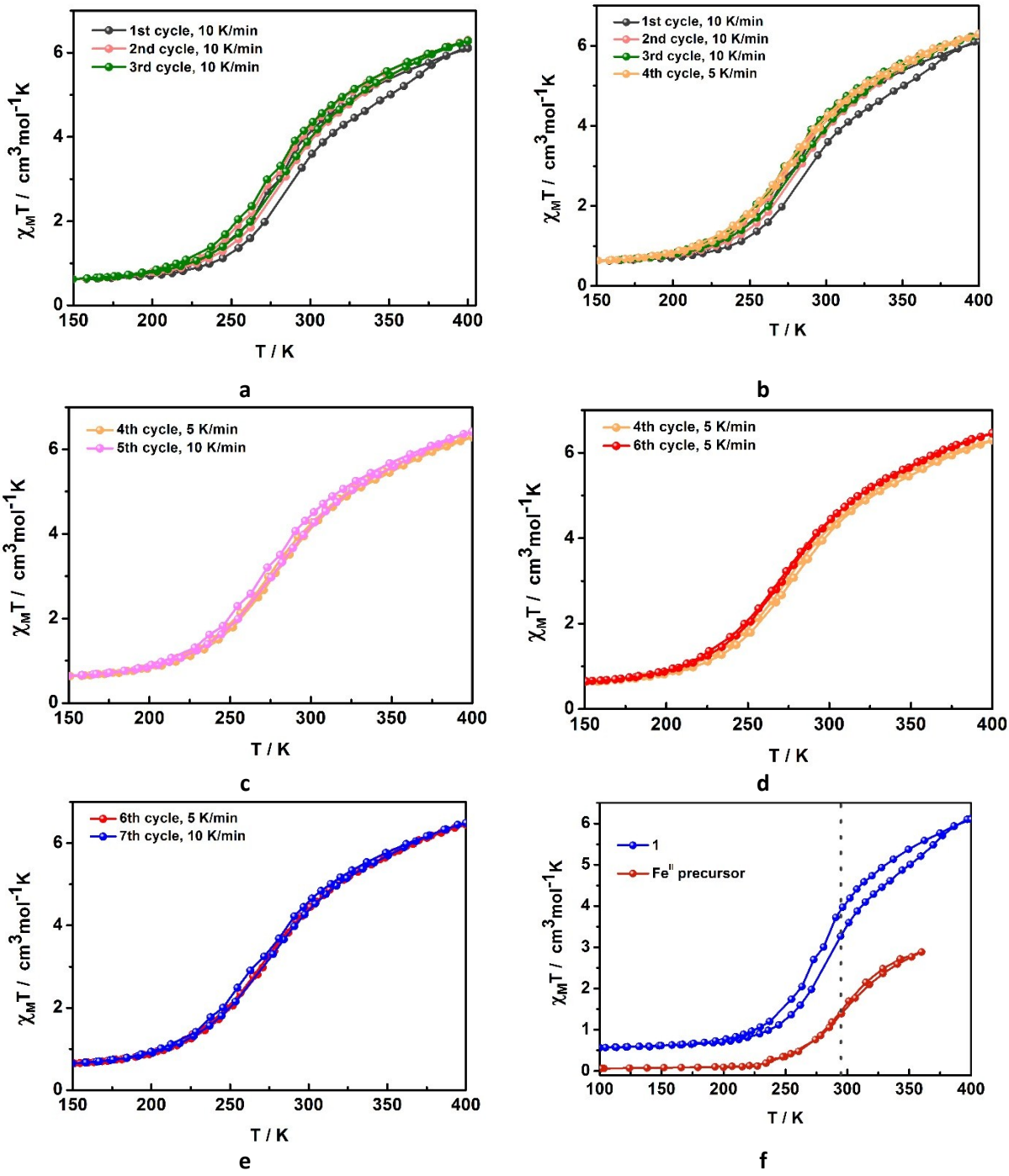

Figure S5 Thermal variation of $\chi_M T$ versus T plot for **1** over cycles with different heating rates (a-e), f) comparison of magnetic profiles for **1** and $[Fe^{II}(3,5\text{-}Me_2TPM)(TPM)][ClO_4]_2$, the cationic precursor.

Table S6 Spin transition temperature of **1** at diffferent cycle and heating rates

Cycles	$T\downarrow$/K	$T\uparrow$/K	Rate/Kmin^{-1}	ΔT/K	χ_MT/cm^{3}mol^{-1}K at 400 K
1st	283.5	293.5	10	10	6.12
2nd	281	287	10	6	6.30
3rd	278	285	10	7	6.28
4th	277.5	280.5	5	3	6.28
5th	273	279	10	6	6.41
6th	273	275	5	2	6.45
7th	270.5	275.5	10	5	6.49

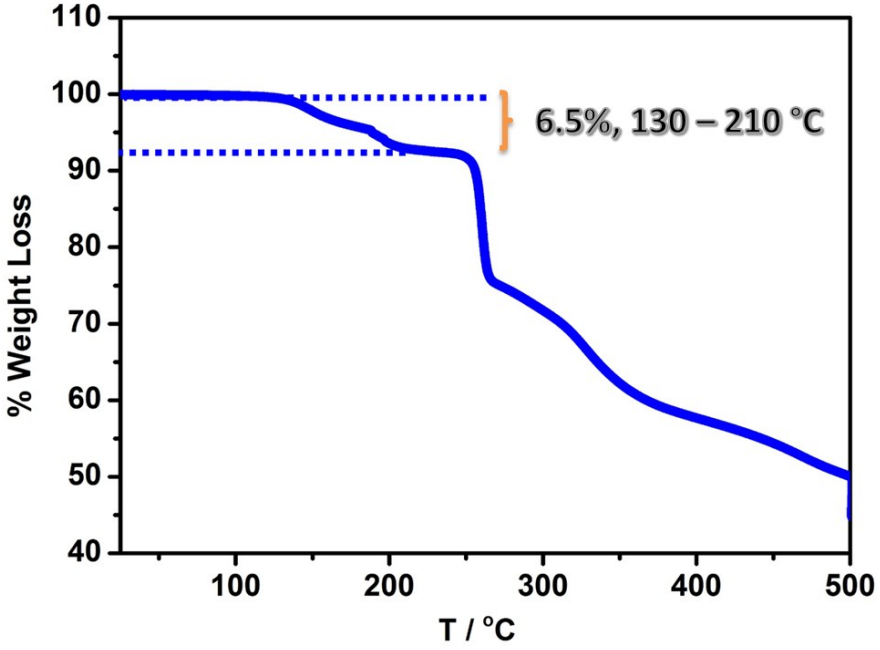
110
100
90
80
70
60
50
40
% Weight Loss
100
200
300
400
500
T / °C
6.5%, 130 – 210 °C

a

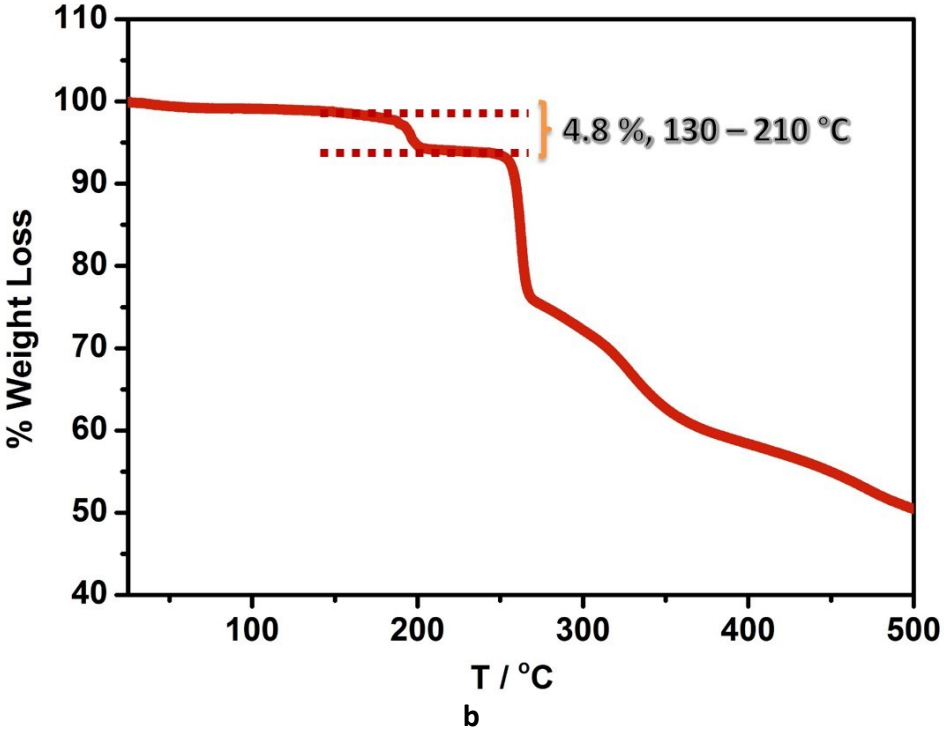
110
100
90
80
70
60
50
40
% Weight Loss
100
200
300
400
500
T / °C
4.8 %, 130 – 210 °C

b

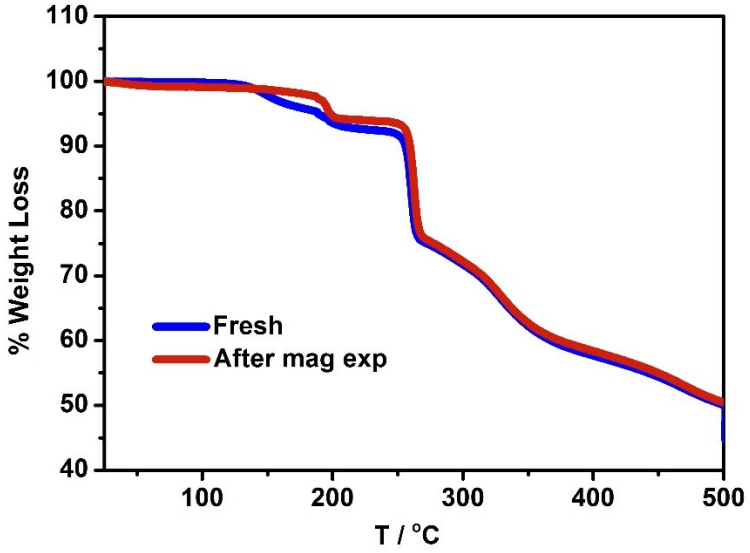

Figure S6 TGA result for compound **1** a) fresh sample (calc. for 2MeCN = 6.67 %), b) after magnetic measurement over 7 cycles (calc. for 1.4MeCN = 4.78 %) c) comparison between a) and b) plots.

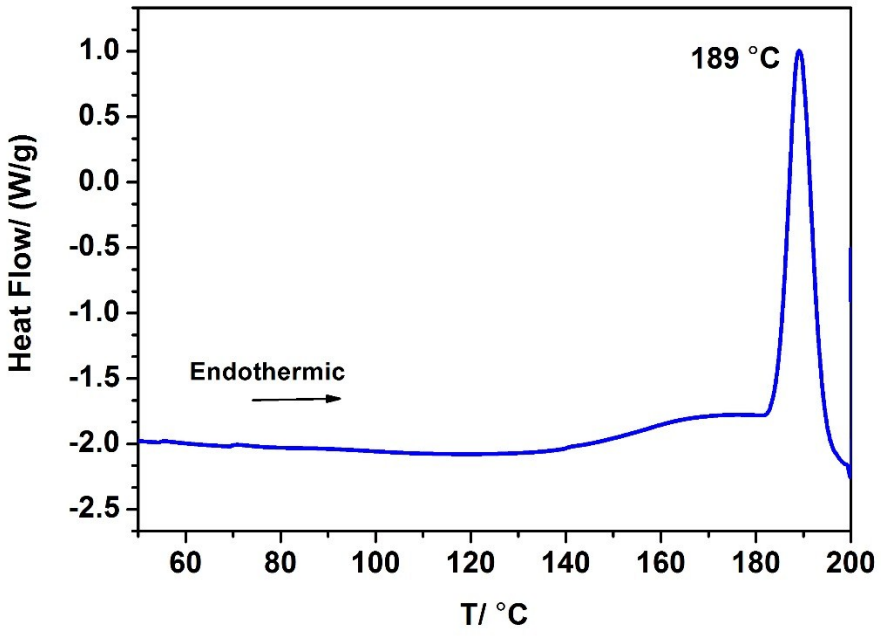

Figure S7 DSC plot for compound **1**

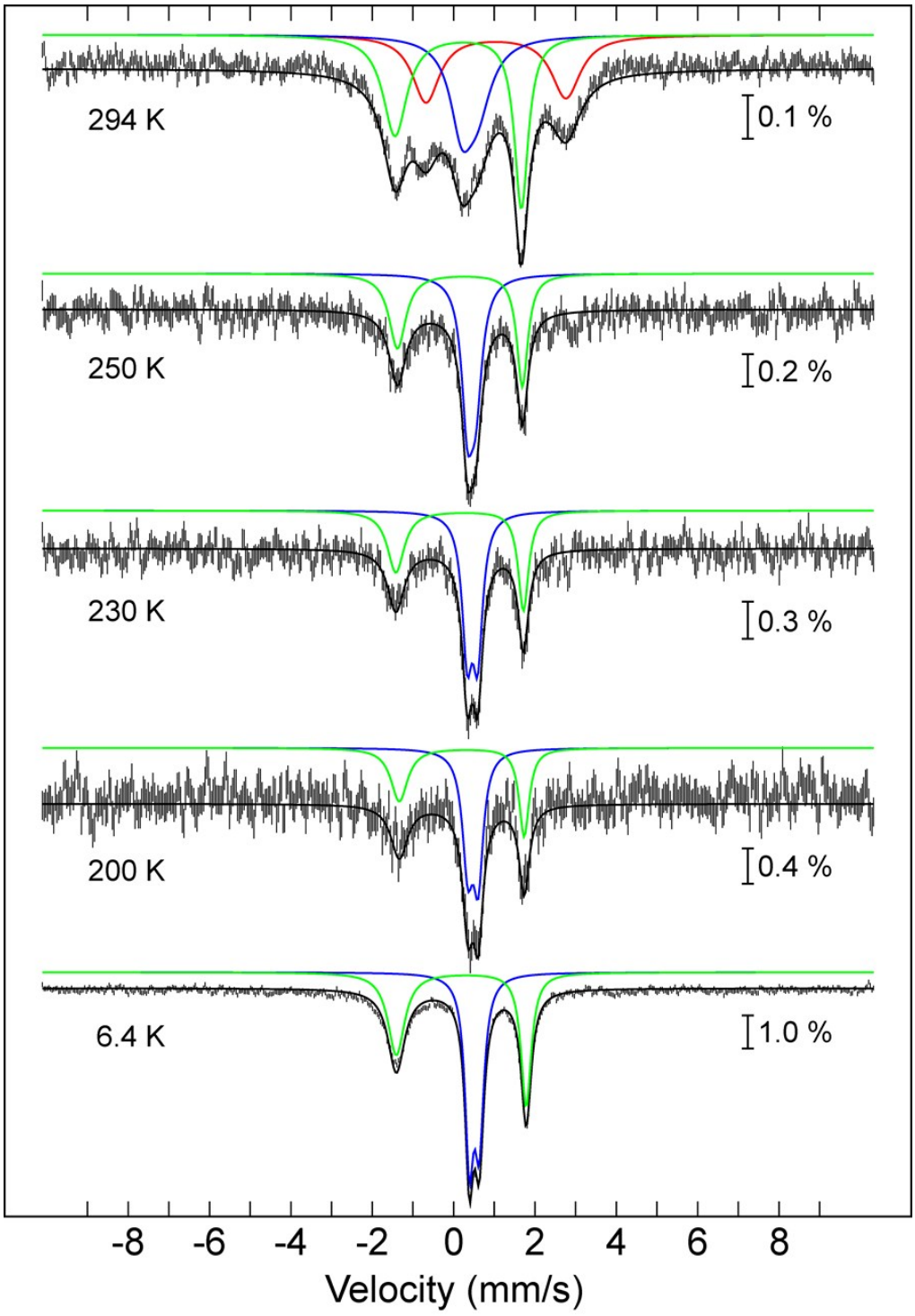

Figure S8 Temperature dependent ^{57}Fe Mössbauer spectra of **1** showing the fitted sub spectra (see Table S7 for parameters)

Table S7 ^{57}Fe Mössbauer spectral parameters for **1**

T (K)	Species	δ (mm/s)	ΔE_Q (mm/s)	Γ_L (mm/s)	Γ_R (mm/s)	I (%)
294	HS Fe^{II}	1.04	3.44	0.81	0.87	40
	LS Fe^{III}	0.11	3.11	0.71	0.41	30
	LS Fe^{II}	0.39	0.39	0.67	0.83	30
250	LS Fe^{III}	0.16	3.07	0.50	0.33	47
	LS Fe^{II}	0.44	0.21	0.34	0.38	53
230	LS Fe^{III}	0.15	3.14	0.50	0.31	44
	LS Fe^{II}	0.46	0.26	0.30	0.30	56
200	LS Fe^{III}	0.20	3.07	0.50	0.30	43
	LS Fe^{II}	0.48	0.26	0.32	0.30	57
6.4	LS Fe^{III}	0.19	3.19	0.50	0.31	49
	LS Fe^{II}	0.51	0.24	0.25	0.28	51

Bulk synthesis of $K[Fe^{III}(azp)_2]\cdot(H_2O)_3\cdot MeOH$ ("1D chain structure"); see ref. 6. For "dimer" structure see ref 3.

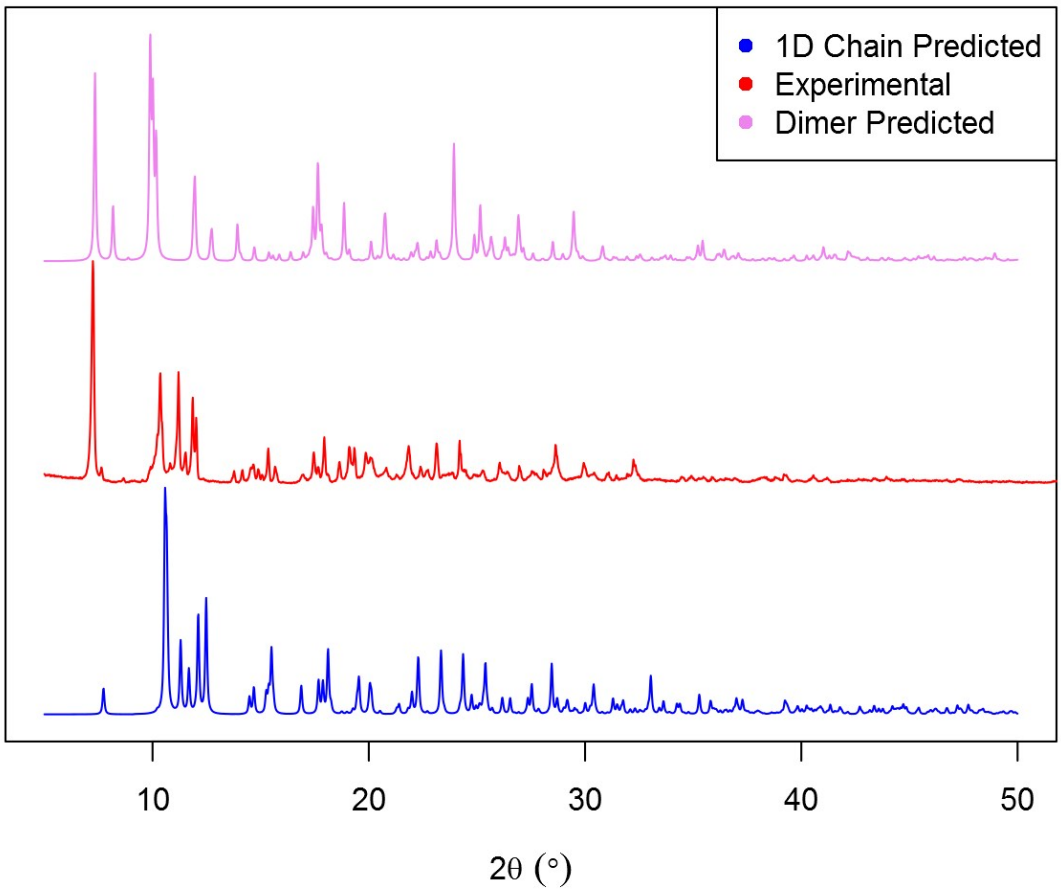

Figure S9 Predicted powder X-ray diffraction patterns of $K[Fe^{III}(azp)_2]\cdot(H_2O)_3\cdot MeOH$ (1D chain)[6] and $K[Fe^{III}(azp)_2]\cdot MeOH\cdot Et_2O$ (dimer),[3] respectively, with the experimental powder pattern of the bulk sample. Clearly a mixture of the phases is formed without any other impurity.

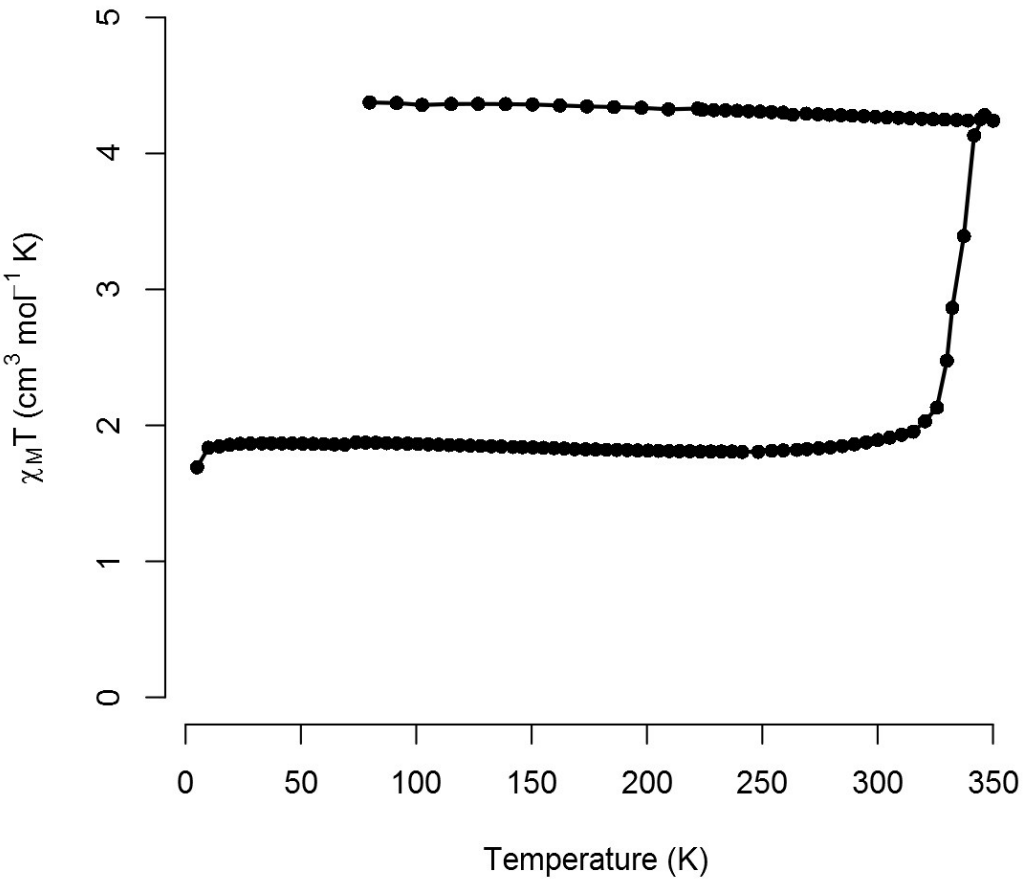

Figure S10 Plot of $\chi_M T$ vs.T for the bulk sample of K[Fe^{III}(azp)$_2$]·(H$_2$O)$_3$·MeOH that gives the PXRD in Figure S9. The plot starts at 2 K, then the sample is warmed up to 350 K followed by cooling down to 70 K.

The Curie-like plateau below 300 K has a higher $\chi_M T$ than expected for LS Fe^{III} probably indicative of some HS form present. The sharp increase at ~340 K is likely due to SCO. Then the platea at 4.2 cm^{3}mol^{-1} K, seen on cooling, is indicative of HS Fe^{III}. We don't know if a phase change has occurred and/or with solvent loss.

References

1. T. M. McPhillips, S. E. McPhillips, H.-J. Chiu, A. E. Cohen, A. M. Deacon, P. J. Ellis, E. Garman, A. Gonzalez, N. K. Sauter, R. P. Phizackerley, S. M. Soltis and P. Kuhn, *J. Synchrotron Radiat.*, 2002, **9**, 401-406.
2. W. Kabsch, *J. Appl. Crystallogr.*, 1993, **26**, 795-800.
3. K. Takahashi, K. Kawamukai, M. Okai, T. Mochida, T. Sakurai, H. Ohta, T. Yamamoto, Y. Einaga, Y. Shiota and K. Yoshizawa, *Chem. Eur. J.*, 2016, **22**, 1253-1257.
4. B. Moubaraki, B. A. Leita, G. J. Halder, S. R. Batten, P. Jensen, J. P. Smith, J. D. Cashion, C. J. Kepert, J.-F. Letard and K. S. Murray, *Dalton Trans.*, 2007, 4413-4426.

5. K. V. Langenberg, *Hons. Thesis, Monash University, Australia*, 1993.
6. W. Phonsri, D. S. Macedo, B. A. I. Lewis, D. F. Wain and K. S. Murray, *Magnetochemistry*, 2019, **5**, 37.